Influence from the Free Volume on the Photoinduced Birefringence in Azocompound-Containing Polymers

Fernando F. Dall'Agnol,*,† O. N. Oliveira, Jr.,‡ and José A. Giacometti§

Departamento de Física, Universidade Estadual do Centro Oeste (Unicentro), R. Simeão Camargo Varela de Sá, 03, Guarapuava, CP 3010 85040-080, Brazil; Instituto de Física de São Carlos, USP, CP 369, 13560-970, São Carlos, SP, Brazil; and Faculdade de Ciências e Tecnologia, UNESP, CP 467, 19060-900, Presidente Prudente, SP, Brazil

Received December 5, 2005; Revised Manuscript Received May 5, 2006

ABSTRACT: The photoinduced birefringence is analyzed in a guest−host azobenzene-containing polymer in the temperature range from 20 to 330 K. An anomalous behavior arises in the low-temperature range, suggesting strong influence from the free volume for the chromophores in the polymer. This influence is so strong that quenched samples have a photoinduced signal ca. 5 times greater than the annealed ones at room temperature. An extended free volume model is presented based on two assumptions about thermal fluctuations in the cavities and their size distribution. This model, which is an extension of the model by Mita et al., can explain the main features of the photoinduced birefringence as a function of time, temperature, and initial free volume state. To account for the influence of free volume on the photoorientation, the detailed reorientation model by Sekkat's was used. We show that Sekkat's model leads to an exponential behavior at small orientation regimes, which simplifies the mathematical treatment and allows the mean free volume to be obtained from the data fitting.

1. Introduction

The trans → cis → trans photoisomerization of azobenzene derivatives leading to photoinduced birefringence[1] in polymer films has been extensively investigated and may be exploited in optical storage,[2] surface-relief gratings,[3] second and third harmonic generation, optical switching,[4] etc. An overview of photoisomerization in azocompound-containing polymers has been produced by Sekkat and Knoll in ref 5. Azobenzene derivatives have also been used as photoprobes for investigating the microstructure and microenvironment in polymers. For example, photoisomerization is suppressed when the free volume available for the chromophores is reduced due to cross-linking in epoxy resins.[6,7] Several models and phenomenological equations have been used to explain photoinduced birefringence, which include Kohlrausch−Williams−Watts[8] and biexponential functions.[9] One successful model was developed by Sekkat et al.,[10] in which the photoisomerization and the angular distribution of the azobenzene groups in the sample are taken into account. In the low-light intensity regime, Sekkat's model leads to biexponential functions in agreement with experimental results. However, the latter model was not conceived to account for the temperature dependence of photoinduced birefringence. Recently, we reported in a letter[11] an orientation model for the temperature dependence to account for the alignment. Here we present the full details of the model and results, in which the Mita et al.[12] free volume model is extended to explain the dynamics of the photoinduced birefringence in a guest−host system of the polymer polystyrene (PS) doped with the dye Disperse Red-1 (DR1). The dynamics of the photoinduced birefringence was analyzed in the range from 20 to 330 K and with two initial free volume states. We also show that photoinduced birefringence can exist at very low temperatures, corroborating an earlier report of photoisomerization at temperatures as low as 4 K.[13]

This extended free volume model is based on the Sekkat's simplified model, i.e, a small molecular angular redistribution, and on two assumptions associated with the thermal fluctuations of the local free volume and the free volume distribution. The efficiency with which azobenzene groups suffer photoisomerization from trans to cis depends on the volume of the nanocavity that contains a chromophore. Expressions are obtained to account for the kinetics of photoinduced birefringence at low light intensity condition. Theoretical and experimental data on films of polystyrene doped with DR1 are compared.

2. Extended Free Volume Model

Photoisomerization processes lead to molecular reorientation that modifies the direction and the modulus of the induced dipole moment. The reorientation mechanism implies in an optical absorption change and in photoinduced birefringence.[10] Here we aim at explaining the mechanisms for photoisomerization and reorientation processes in polymer matrices, focusing on the influence of the polymer free volume, which is done with an extended free volume model. Two assumptions were made that do not constitute any new paradigms, for their contents have been used by other authors with small variations.[12,14]

2.1. First Assumption. The first assumption is that the volumes of the cavities suffer thermal fluctuations and may be described by a Gaussian function centered at the average volume, V_M. The normalized probability of finding the cavity with volume between V and $V + dV$ is given by

$$P(V)\,dV = \frac{1}{\sqrt{\pi}\Delta V}\exp\left[-\left(\frac{V - V_M}{\Delta V}\right)^2\right]dV \qquad (1)$$

where ΔV is a width parameter that is assumed to increase

† Universidade Estadual do Centro Oeste (Unicentro).
‡ Instituto de Física de São Carlos, USP.
§ Faculdade de Ciências e Tecnologia, UNESP.
* Corresponding author. E-mail: dallangol@unicentro.br.

10.1021/ma052604z CCC: $33.50
Published on Web 06/15/2006

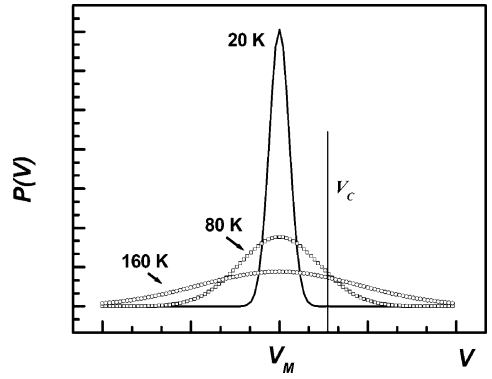

Figure 1. Probability density distribution of finding a cavity with a given volume. The probability function is centered at V_M, and V_C is the critical volume. Functions are shown for three temperatures: 20, 80, and 160 K.

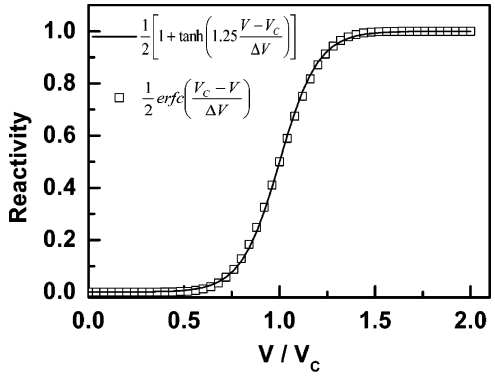

Figure 2. Comparison between reactivity curves for the complementary error function and a hyperbolic tangent function for a typical value of V_C and ΔV.

linearly with the temperature (thermal energy) as

$$\Delta V(T) = \Delta V_0 T \tag{2}$$

with ΔV_0 being a thermal fluctuation coefficient given in units of m^3/K. The probability density as a function of the cavity volume is shown in Figure 1 for three temperatures. There is a nonzero probability for each cavity to be larger or smaller than a critical value, V_C. The critical value defines the volume above which isomerization of the azobenzenic group is possible. In cavities smaller than V_C isomerization cannot occur due to steric hindrance. V_C is expected to be different for distinct azobenzenic molecules.[15]

The probability of finding a cavity with a volume larger than V_C is known as the reactivity function Φ, given by

$$\Phi(V_M) = \frac{\frac{1}{\pi\Delta V}\int_{V_C}^{\infty}\exp\left[-\left(\frac{V-V_M}{\Delta V}\right)\right]}{\frac{1}{\pi\Delta V}\int_{-\infty}^{\infty}\exp\left[-\left(\frac{V-V_M}{\Delta V}\right)\right]} = \frac{1}{2}\,\mathrm{erfc}\left(\frac{V_C-V_M}{\Delta V}\right) \tag{3}$$

The erfc($-x$) function can be approximated by another function involving tanh(x), as follows.

$$\mathrm{erfc}\left(\frac{V_C-V_M}{\Delta V}\right) \cong \frac{1}{2}\left\{1+\tanh\left[1.25\left(\frac{V_M-V_C}{\Delta V}\right)\right]\right\} \tag{4}$$

where the factor 1.25 was found to yield the best fitting between the two functions. Figure 2 demonstrates how good the approximation is for $V_C = 1$ and $\Delta V = 0.25$, and this applies to other typical values of V_C and ΔV. The transformation in eq 4 is convenient because, computationally, it is much quicker to employ tanh than the erfc function.

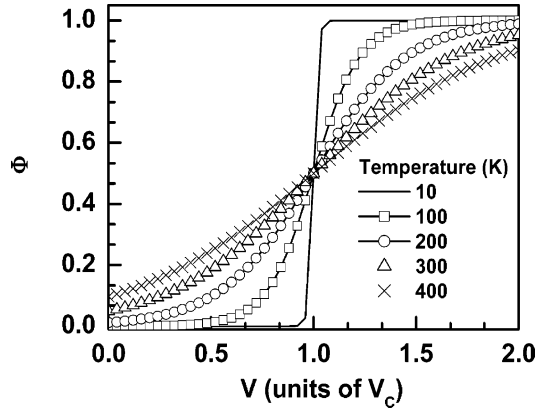

Figure 3. Reactivity curves Φ as a function of cavity volume, for five temperatures: 10, 100, 200, 300, and 400 K.

Then, our first assumption is defined as follows: The reactivity of an azobenzenic molecule contained in a cavity with an average volume V_M is given by $\Phi(V) = {}^1/_2(1 + \tanh[1.25((V_M - V_C)/\Delta V)])$.

Figure 3 shows the reactivity curve for five temperatures. For cavities with $V_M \ll V_C$, $\Phi \to 0$ and for $V_M \gg V_C$, $\Phi \to 1$, as expected. As the temperature increases, the reactivity curve is broadened in such a way that for $V < V_C$ the reactivity increases with temperature while for $V > V_C$ it decreases. At 0 K, where no thermal fluctuations takes place ($\Delta V \to 0$), the reactivity becomes a step function at V_C. Note that the reactivity $\Phi(V_M)$ is not the probability of isomerization for an azobenzenic molecule, but the probability of an azobenzenic molecule to be allowed to isomerize. The first assumption gives a precise definition for the critical volume V_C, i.e., the volume in which the probability of isomerization of an azobenzenic molecule is equal to ${}^1/_2$.

The reactivity is never zero, even though it is negligible when $V_C - V_M$ is much larger than ΔV. A nonzero reactivity even for $V = 0$ is physically acceptable, since glassy polymers are known to exhibit constant molecular rearrangement, which creates cavities where there was none, thus allowing isomerization of chromophores that were trapped in these places. Furthermore, to allow nonzero reactivity in regions with no local free volume is convenient to describe the contribution of these molecules, mainly at high temperatures close to the glass transition temperature, where the molecular rearrangement is fast and thermal fluctuations are large.

2.2. Second Assumption. In a paper in 1977, Robertson[16] suggested a normalized Gamma distribution function $\xi(V)$ to describe the free volume distribution:

$$\xi(V_M) = \frac{\lambda}{\Gamma(\alpha)V_T}\left(\lambda\frac{V_M}{V_T}\right)^{\alpha-1}\exp\left(-\lambda\frac{V_M}{V_T}\right) \tag{5}$$

where V is the average volume of the cavity, $\Gamma(x)$ is the gamma function, V_T is the total free volume, and α and λ are adjustable parameters. In terms of the average free volume for all cavities $\bar{V}$, eq 5 becomes

$$\xi(V_M) = \frac{\alpha^\alpha}{\Gamma(\alpha)\bar{V}}\left(\frac{V_M}{\bar{V}}\right)^{\alpha-1}\exp\left(-\alpha\frac{V_M}{\bar{V}}\right) \tag{6}$$

where $\bar{V} = \alpha V_T/\lambda$ is obtained by the integral $\bar{V} = \int_0^\infty V_M\xi(V_M)\,dV_M$. It is important not to mistake the average free volume of

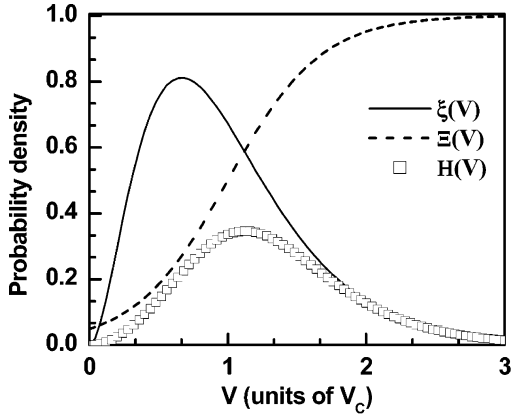

Figure 4. Typical curves of the free volume distribution (ξ), the participativity function (Ξ), and the participation function ($H = \xi\Xi$) of the chromophores.

the distribution ξ, represented by $\bar{V}$, with the average volume of a single cavity, V_M. From now on the index "M" in V_M will be suppressed. The distribution in eq 6 has the general features expected for the cavity's volume. It is a well-behaved, smooth normalized function, has boundary conditions of $\xi(0) = 0$ and $\xi(\infty) = 0$, and tends rapidly to zero. Since the exact evaluation of such a distribution is not possible, any function presenting these features is sufficient to describe approximately the free volume influence whatever the exact distribution should be. In this work, we assume that the cavity size distribution is given by a Poisson function where $\alpha = 3$ in eq 6. Thus, $\xi(V)$ can be taken as

$$\xi(V) = \frac{27}{2\bar{V}}\left(\frac{V}{\bar{V}}\right)^2 \exp\left(-\frac{3V}{\bar{V}}\right) \tag{7}$$

The second assumption is summarized by stating that azobenzenic molecules are uniformly distributed in cavities in the polymers, whose volume distribution is given by $\xi(V)$ as in eq 7. The solid line in Figure 4 shows a typical curve for the cavity size distribution given by eq 7. It should be stressed that the meaning of the volume "V" in ξ is not well-defined because certainly the cavities are not spheres. The cavities are expected to have a variety of shapes so that large cavities with a cylindrical shape may allow isomerization as much as a small spherical cavity. This does not alter the assumption in its essence. It suffices to reinterpret the volume of the cavities as effective volumes, i.e., the largest spherical volume inscribed to the cavity, and the adjustable parameter $\bar{V}$ can be understood as the effective average free volume of the polymer.

3. Applying the Model to Photoinduced Birefringence

To treat the photoinduced birefringence, we must consider not only the photoisomerization but also the reorientation mechanism. It is convenient in this case to introduce two new functions, namely the participativity (Ξ) and participation (H) functions. The participativity function appears naturally from the solutions of the differential equations describing the time evolution of the photoinduced birefringence. It has different expressions for the trans and cis states, being defined as

$$\Xi_T = \frac{\varphi_T}{\chi_T}\Phi[1 - \exp(-\chi_T t_F)] \tag{8}$$

and

$$\Xi_C = \frac{\varphi_C}{\chi_C}[1 - \exp(-\Phi\chi_C t_F)] \tag{9}$$

where Ξ_T and Ξ_C are the participativity of the molecules in trans and cis states, respectively, φ_T is the light-driven rate for transition to the aligned trans state, φ_C is the light-driven rate for transition to the aligned cis state, χ_T is the loss rate due to thermally activated angular diffusion of the aligned molecules in trans, χ_C is the loss rate due to thermally activated back-reaction from cis aligned to trans unaligned, and t_F is the time interval during which the pump light was on.

In the same way that the reactivity describes how difficult it is for the isomerization to occur, the participativity function is associated with the difficulty in the angular reorientation process. This function increases with the photoisomerization time exhibiting a threshold as time tends to infinite. Low light intensities and high loss in alignment reduce the participativity of the chromophores. The temperature may change the mobility and affect the participativity of the chromophores. Note that less reactive chromophores are also less participative in the photoinduced birefringence. All of this is encompassed by eqs 8 and 9. For the trans molecules, the reactivity appears as a multiplicative factor. For the molecules in cis state it appears multiplying only the characteristic time. The participativity function varies between 0 and 1. Chromophores in small cavities, with little mobility to isomerize and reorientate, are less participative. On the other hand, in large cavities chromophores are very participative. However, large cavities are rare. The contribution to the birefringence depends on both how participative the chromophores are and how numerous the cavities that contain them are. This leads us to another convenient parameter, defined as the product of the participativity Ξ and the cavity size distribution ξ. This quantity will be referred to as *participation* and represents the contribution to the birefringence from all chromophores contained in cavities with volume between V and $V + dV$. Figure 4 shows a typical curve of the ξ, Ξ, and the participation $H = \xi\Xi$ of the chromophores. The area under the participation function is proportional to the birefringence.

3.1. Angular Reorientation Model. We obtain an analytic treatment for the birefringence with the free volume influence by reducing the system to only three states, referred to as "states of alignment", defined by the following equation:

$$T_O \cong 1 \tag{10}$$

$$T_{||},\ C_{||} = \int_0^{2\pi}\int_0^{\pi} f_{T,C}(\theta,\phi)\sin\theta\cos^4\theta\, d\theta\, d\phi \tag{11}$$

where $f_{T,C}(\theta,\phi)$ is the angular distribution of the molecules in trans or cis states; θ and ϕ are the polar and azimuth angles, respectively. T_O is the state of molecules in trans unaligned; $T_{||}$ and $C_{||}$ are the states of alignment for the molecules in trans and cis states, respectively. As defined by eq 11, the birefringence is proportional to a linear combination of $T_{||}$ and $C_{||}$. The distribution, $f(\theta,\phi)$, can be evaluated by many models that account for the angular reorientation of the chromophores.[10,17] For a system in the presence of a pump light the states of alignment and their transition are represented in Figure 5 for the chromophores in cavities with volume between V and $V + dV$. In this figure, φ_T, φ_C are the light-driven rates from $T_O \rightarrow T_{||}$, $T_O \rightarrow C_{||}$, χ_T is a thermal diffusion rate for $T_{||} \rightarrow T_O$, and χ_C is the thermal back-reaction $C_{||} \rightarrow T_O$.

The photoinduced transition trans $\rightarrow$ cis and the spontaneous decay cis $\rightarrow$ trans of the chromophores depend on the size of

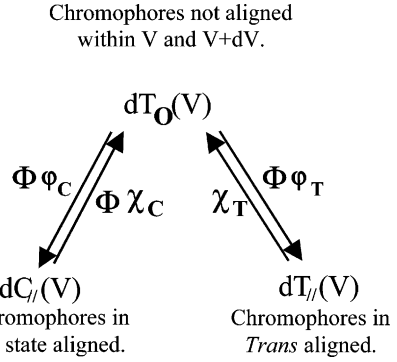

Figure 5. Diagram for the transitions between the alignment states T_O, $T_{||}$, and $C_{||}$ for chromophores in cavities with volume between V and $V + dV$.

the cavity. So, the transition rates must be weighted by the reactivity, which results in new rates, viz. $\Phi\varphi_T$, $\Phi\varphi_C$, and $\Phi\chi_C$. In other words, the chromophores in cavities with volume between V and $V + dV$ will populate state $C_{||}$ with a rate $\Phi\varphi_C$ and the state $T_{||}$ with rate $\Phi\varphi_T$. The rate for the loss of alignment due to angular thermal diffusion occurs not only with the chromophores but also with the polymer matrix. Even when prevented from moving independently, chromophores may lose their alignment together with the movement of the polymer chains. In this case we assume that the thermal diffusion rate χ_T does not depend on the volume of the cavity and therefore is not weighted by the reactivity function. Thermal diffusion rates are assumed to have an Arrhenius dependence with temperature.[18] Furthermore, we assume that the angular thermal diffusion does not depend on the initial free volume, which is reasonable since thermal expansion is very small. With this approximation, quenched and annealed samples have the same angular diffusion rates.

By assuming eq 10, the chromophores must have a very small alignment so that the state T_O remains practically unchanged in time. This implies that the rates for birefringence buildup, φ_T and φ_C, must be much smaller than the rates of the birefringence decay, χ_T and χ_C. This condition can be obtained experimentally with low pump light intensities.

3.2. Buildup of the Photoinduced Birefringence. According to the second assumption in section 2.2, the number of molecules in cavities with volume between V and $V + dV$ is

$$dT_O(V) = T_O\xi(V)\,dV \tag{12}$$

From the model depicted in Figure 5 we can establish the rate equations that describe the buildup of the birefringence:

$$\frac{\partial(dT_O)}{\partial t} \cong 0 \tag{13}$$

$$\frac{\partial(dT_{||})}{\partial t} = \Phi\varphi_T\,dT_O - \chi_T\,dT_{||} \tag{14}$$

$$\frac{\partial(dC_{||})}{\partial t} = \Phi\varphi_C\,dT_0 - \Phi\chi_C\,dC_{||} \tag{15}$$

Using eq 12 in eqs 14 and 15 and solving the differential equations, with the approximations discussed in section 3.1, we obtain

$$dT_{||} = \frac{\varphi_T}{\chi_T}\Phi(1 - e^{-\chi_T t})T_O\xi\,dV \tag{16}$$

$$dC_{||} = \frac{\varphi_C}{\chi_C}(1 - e^{-\Phi\chi_C t})T_O\xi\,dV \tag{17}$$

An element of birefringence is given by the linear combination of eqs 16 and 17, which results in

$$d\Delta n_B = A_T\,dT_{||} + A_C\,dC_{||} \tag{18}$$

where $d\Delta n_B(V)$ is the buildup of the birefringence; A_T and A_C are the amplitudes corresponding to the trans and cis states, respectively. A_T and A_C are adjustable parameters.

Integrating eq 18 using eqs 16 and 17, we obtain

$$\Delta n_B = A_T\frac{\varphi_T}{\chi_T}(1 - e^{-\chi_T t})\int_0^\infty \xi\Phi\,dV + A_C\frac{\varphi_C}{\chi_C}\int_0^\infty \xi(1 - e^{-\Phi\chi_C t})\,dV \tag{19}$$

As a function of the participativity eq 19 becomes

$$\Delta n_B = A_T\int_0^\infty \Xi_T\xi\,dV + A_C\int_0^\infty \Xi_C\xi\,dV \tag{20}$$

3.3. Decay of the Birefringence. In absence of light the photoorientation rates φ_T and φ_C are null, and the equations for the decay of birefringence are given by

$$\frac{\partial(dT_{||})}{\partial t} = -\chi_T\,dT_{||} \tag{21}$$

$$\frac{\partial(dC_{||})}{\partial t} = -\chi_C\Phi\,dC_{||} \tag{22}$$

whose solutions are

$$dT_{||} = (dT_{||})_0 e^{-\chi_T t} \tag{23}$$

$$dC_{||} = (dC_{||})_0 e^{-\chi_C\Phi t} \tag{24}$$

The initial amplitudes $(dT_{||})_0$ and $(dC_{||})_0$ are induced in the time formation, t_F. They are given by eqs 16 and 17. The decay of birefringence is obtained by integrating the linear combination of eqs 23 and 24:

$$\Delta n_D = A_T\frac{\varphi_T}{\chi_T}(1 - e^{-\chi_T t_F})\int_0^\infty \Phi\xi\,dV\,e^{-\chi_T t} + A_C\frac{\varphi_C}{\chi_C}\int_0^\infty (1 - e^{-\Phi\chi_C t_F})e^{-\Phi\chi_C t}\xi\,dV \tag{25}$$

As a function of the participativity, we obtain

$$\Delta n_D = A_T\int_0^\infty \Xi_T(t_F)e^{-\chi_T t}\xi\,dV + A_C\int_0^\infty \Xi_C(t_F)e^{-\Phi\chi_C t}\xi\,dV \tag{26}$$

3.4. Experimental Details. The birefringence values were calculated from changes in transmission using the traditional setup[19] shown in Figure 6, with an Ar^+ laser (514 nm polarized light, 15 mW/cm^2) inducing orientation of azobenzene groups. A low-power He−Ne laser (632.8 nm, 2.2 mW) modulated at 1000 Hz with a chopper was used to probe the photoisomerization process. The response signal was measured with a photodetector and a lock-in amplifier. The relation between

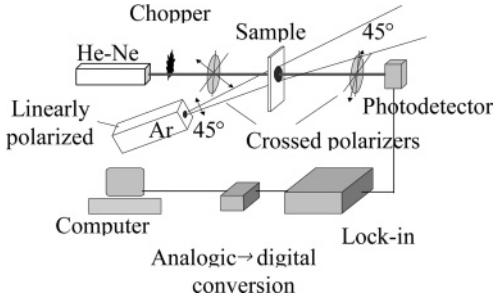

Figure 6. Experimental setup for measuring photoinduced birefringence.

birefringence Δn and the measured intensity is given by[20]

$$\frac{I}{I_0} = \sin^2\left(\frac{\pi \Delta n L}{\lambda}\right) \tag{27}$$

where I and I_0 are the measured probe intensities before and after the probe beam had passed across the analyzer, L is the sample thickness, and λ is the light probe wavelength. Guest−host samples were prepared by casting a solution of polystyrene (PS), containing 0.3 wt % of DR1 in chloroform. Prior to the measurements the samples were free of solvent. The thickness of the samples was ~50 μm. Annealed samples were first heated to 393 K and then cooled in steps of 5 K until 343 K. In each cooling step the sample remained during 6 h at the set temperature. Quenched samples were first heated to 393 K and then immersed in a bath of water and ice.

3.5. Results and Predictions of the Model. For an intuitive understanding of the influence of the free volume on the photoinduced birefringence, we shall comment upon a few properties of the chromophores and what happens when the initial free volume and the temperature are varied. In principle, any azobenzenic molecule is photoisomerizable since $\Phi(V)$ is a nonzero function for any cavity volume. However, molecules within very small cavities are assumed not to be isomerizable. The decay processes are governed by an Arrhenius function, which implies that with no free volume influence one would expect the characteristic times to decrease monotonically with temperature. However, according to the first assumption in section 2.1, as the temperature increases thermal fluctuations can turn nonparticipative chromophores into participative ones with small reactivities. Also, molecules in cavities larger than V_C have their reactivity reduced, as seen in Figure 3. In both cases the average reactivity of the participative chromophores is reduced with temperature. So, when fitted with a biexponential function the effective characteristic time for the fast process may grow with temperature for low temperatures. This effect, shown in Figure 8, was measured and predicted by the theory as shown in the solid curve. Actually, the behavior shown in Figure 8 indicates that a biexponential function is not adequate to describe the photoinduced orientation in polymers, as illustrated by the lack of agreement between the experimental data and the model prediction, even for the best parameters found for the whole experimental data.

The amplitude of photoinduced birefringence can also increase with the temperature for low temperatures, in contradiction to an Arrhenius process. According to the second assumption in section 2.2, the free volume distribution is shifted to the right of the critical value as the temperature increases, which implies in more chromophores becoming participative. This effect, shown in Figure 9, was measured for temperatures between 0 and 180 K and is predicted by the theory as the solid curve shows. For sufficiently high temperatures, thermally activated mechanisms predominate and the amplitude decreases with the temperature.

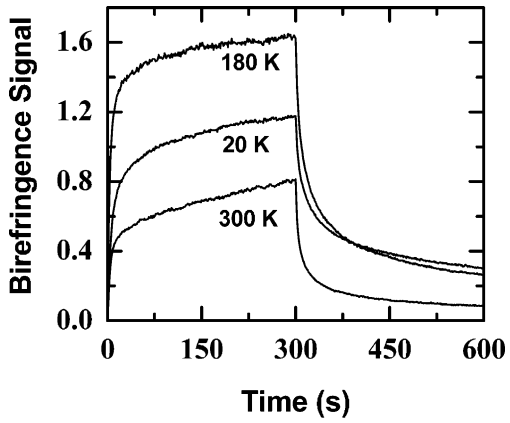

Figure 7. Buildup and decay curves for photoinduced birefringence measured at 20, 180, and 300 K.

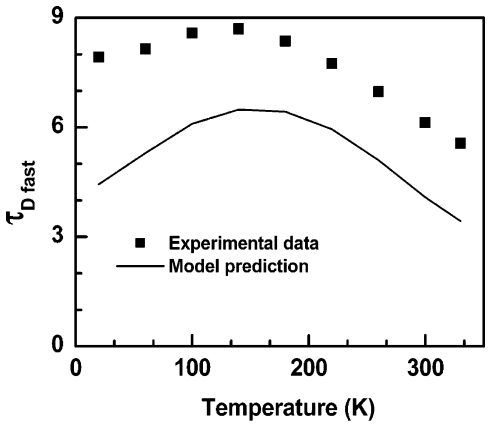

Figure 8. Experimental and theoretical curves for the time constant of the fast decay vs temperature.

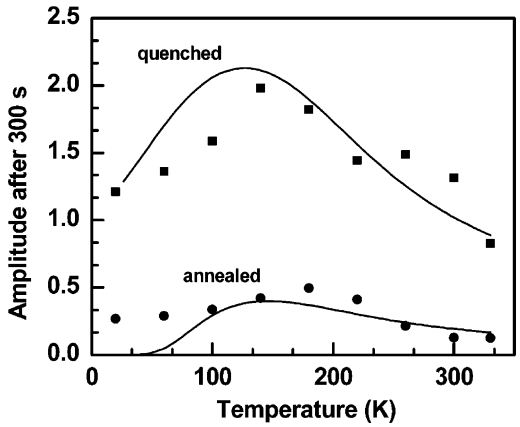

Figure 9. Experimental data and simulations with the model for temperature dependence of the amplitude for quenched and annealed samples.

Finally, quenched samples exhibit higher birefringence amplitudes than the annealed ones. This is because quenched samples have larger average free volume $\bar{V}$, which implies in higher reactivity, participativity, and participation of the chromophores. Consequently, it will exhibit higher amplitudes as observed in Figure 9. The prediction of the model is represented by the solid curve. This is consistent with the results by Sekkat et al.[21] in which the photoorientation amplitude decreased at high pressures, as the mean free volume became smaller.

Table 1. Parameters Used in the Simulations of Curves Shown in Figures 8 and 9

$A_C = 9$	$\chi_{C_\infty} = 10\ s^{-1}$
$A_T = 0.07$	$\chi_{C_0} = 0.25\ s^{-1}$
$\varphi_C = 0.05\ s^{-1}$	$\chi_{T_\infty} = 0.02\ s^{-1}$
$\varphi_T = 0.05\ s^{-1}$	$V_C = 1$
$E_C = 7.8$ kJ/mol	$\bar{V}$(quenched) $= 0.9$
	$\bar{V}$(annealed) $= 0.05$
$E_T = 6$ kJ/mol	$\Delta V_0 = 0.004$

The parameters used in the model should explain the experimental curves with regard to both temporal evolution and amplitude of birefringence, as a function of the temperature. Figures 8 and 9 show the best fitting that matches the time evolution (Figure 7) and the temperature dependence of the photoinduced birefringence. The time evolution curves and their fitting with the model were shown in an early paper.[11] The parameters used are given in Table 1.

4. Extended Free Volume Model for Other Phenomena

The model proposed here is applicable to any phenomena involving isomerization processes in polymers, which include the formation of surface-relief gratings (SRG) and fluorescence, in addition to the optical absorption and photoinduced birefringence treated in this paper. The general procedure to apply it can be easily obtained. Whatever the phenomenon, its dynamics must be a function of the rates of trans to cis conversion and vice versa. The first step is to multiply the rates sensitive to the cavities volume by the reactivity function. Then, the dynamics must be found for the phenomenon associated with chromophores contained in cavities with volumes between V and $V + dV$. Then, one should evaluate the phenomenon amplitude by integrating over the chromophores contained in all cavities, that is, from zero to infinity. The application of this model to other phenomena is underway.

5. Conclusion

In this work we presented an extended free-volume model to account for the isomerization processes in polymers. This model predicts the main features of birefringence and points to the important role played by free volume in measurements of optical absorption and photoinduced birefringence. For the latter, depending on the initial free volume, one could measure differences of more than 500% in the birefringence signal, demonstrating that a model for the photoisomerization mechanisms in polymer matrices will only be accurate if it takes the free volume into account. We believe that the difficulties in fitting the photoinduced birefringence are due to an approximation error in the theoretical model for low temperatures. The rates for the birefringence decay, χ_T and χ_C, should be much larger than the rates φ_T and φ_C that induce the birefringence. That is an important approximation that keeps most of the chromophores unaligned. But at very low temperatures, the thermally activated rates χ_T and χ_C become much smaller so that $\varphi_{T,C} \approx \chi_{T,C}$. Then, the photoinduced alignment of the photoisomerizable molecules is large, causing the birefringence to saturate, and this is not taken into account in the model. To explain saturation of the photoinduced birefringence at low temperatures, one should consider the angular dependence in the reorientation process, which was neglected in this model. A theoretical model, taking angular distribution and free volume into account, is being developed.

Acknowledgment. Financial assistance from FAPESP, CAPES, CNPq, and IMMP/MCT (Brazil) is acknowledged.

References and Notes

(1) Todorov, T.; Nicolova, L.; Tomova, N. *Appl. Opt.* **1984**, *23*, 4309−4312.
(2) Dhanabalan, A.; Mendonça, C. R.; Balogh, D. T.; Misoguti, L.; Constantino, C. J. L.; Giacometti, J. A.; Zílio, S. C.; Oliveira, O. N., Jr. *Macromolecules* **1999**, *32*, 5277−5284.
(3) Kim, D. Y.; Tripaty, S. K.; Li, L.; Kumar, J. *Appl. Phys. Lett.* **1995**, *66*, 1166−1168.
(4) Sekkat, Z.; Knoesen, A.; Lee, V. Y.; Miller, R. D. *J. Phys. Chem. B* **1997**, *101*, 4733.
(5) Sekkat, Z.; Noll, W. *Photoreactive Organic Thin Films*; Academic Press: New York, 2001.
(6) Chin, In-Joo; Sung, C. S. P. *Macromolecules* **1984**, *17*, 2603−2607.
(7) Sung, C. S. P.; Pyun, E.; Sun, H.-L. *Macromolecules* **1986**, *19*, 2922−2932.
(8) Williams, G.; Watts, D. C. *Trans. Faraday Soc.* **1970**, *66*, 80−85.
(9) Xu, G.; Si, J.; Liu, X.; Yang, Q. G.; Ye, P.; Lie, Z.; Shen, Y. *J. Appl. Phys.* **1999**, *85*, 681−684.
(10) Sekkat, Z.; Wood, J.; Knoll, W. *J. Phys. Chem.* **1995**, *99*, 17226−17234.
(11) Dall'Agnol, F. F.; Silva, J. R.; Zílio, S. C.; Oliveira, O. N., Jr.; Giacometti, J. A. *Macromol. Rapid Commun.* **2002**, *23*, 948−951.
(12) Mita, I.; Horie, K.; Hirao, K. *Macromolecules* **1989**, *22*, 558−563.
(13) Yoshii, K.; Mashida, S.; Horie, K.; Itoh, M. *J. Non-Cryst. Solids* **2000**, *272*, 75−84.
(14) Naito, T.; Horie, K.; Mita, I. *Macromolecules* **1991**, *24*, 2907−2911.
(15) Victor, J. G.; Torkelson, J. M. *Macromolecules* **1987**, *20*, 2241−2250.
(16) Robertson, R. E. *J. Polym. Sci., Polym. Symp.* **1977**, *63*, 173−183.
(17) Pedersen, T. G.; Johansen, P. M.; Holme, N. C. R.; Ramanujam, P. S. *J. Opt. Soc. Am. B* **1998**, *15*, 1120−1129.
(18) Silva, J. R.; Dall'Agnol, F. F.; Oliveira, O. N., Jr.; Giacometti, J. A. *Polymer* **2002**, *43*, 3753−3758.
(19) Rochon, P.; Gosselin, J.; Natansohn, A.; Xie, S. *Appl. Phys. Lett.* **1992**, *60*, 4−5.
(20) Mateev, V.; Markovsky, P.; Nilolova, L.; Todorov, T. *J. Phys. Chem.* **1992**, *96*, 3055−3058.
(21) Sekkat, Z.; Kleideiter, G.; Knoll, W. *J. Opt. Soc. Am. B* **2001**, *18*, 1854−1857.

MA052604Z